Journal of the European Ceramic Society 21 (2001) 1187–1194

www.elsevier.com/locate/jeurceramsoc

Nucleation and crystal growth in commercial LAS compositions

M. Guedes [a], A.C. Ferro [c], J.M.F. Ferreira [b,*]

[a] *Department of Mechanical Engineering, EST, IPS, 2914-508 Setúbal, Portugal*
[b] *Department of Ceramics and Glass Engineering, UIMC, University of Aveiro, 3810-193 Aveiro, Portugal*
[c] *Department of Materials, IST, Av. Rovisco Pais, 1, 1000-001 Lisboa, Portugal*

Received 14 September 1999; received in revised form 20 July 2000; accepted 31 July 2000

Abstract

Thermal cycles for crystal nucleation of two commercial compositions of the $Li_2O{\cdot}Al_2O_3{\cdot}SiO_2$ system, Ceran® and Robax®, were determined by DTA. Both glasses show two exothermic peaks, the first peak corresponding to crystallisation from the glassy phase and the second one to a phase transformation. Crystalline phases formed on heating up to the first maximum exothermic peak temperature are a lithium alumino-silicate ($Li_xAl_xSi_{1-x}O_2$) and an unidentified phase, which then transform to β-spodumene, tetragonal silica and an unidentified phase at the second maximum exothermic peak temperature. Kinetic parameters for crystallisation were determined. For both glasses, the Avrami parameter (n) calculated from the Ozawa equation is between 1 and 3, indicating that surface and volume crystallisation occur simultaneously. The activation energies calculated from the Kissinger model yield 195.8 kJ/mol for Ceran® and 113.2 kJ/mol for Robax®. For each glass, the thermal cycle for nucleation was optimised by studying the influence of time and temperature on the position of the maximum crystallisation peak temperature. It was observed that sintering completion requires temperatures higher than the crystallisation onsets, hindering powders' full densification by pressureless sintering.

Keywords: Crystal growth; Glass ceramics; LAS; Microstructure; Nucleation; Sintering

1. Introduction

Glass ceramics are polycrystalline materials formed by controlled crystallisation heat treatments of appropriate parent glasses.[1–6] Their microstructure consists on a high concentration of small crystals, typically 0.1–1 μm,[7] uniformly distributed in a residual glass phase.[2–4]

The crystalline phases formed and the crystals' growth rate and final size depend not only on the chosen parent glass but also on the imposed thermal treatment and on the addition of nucleating agents. The heat treatment comprises nucleation and crystallisation temperature holds, and other holding stages may be included in order to develop the desired structure and properties.[2,4,8] Nucleating agents are minor constituents that provide the desired microstructure by supplying the nuclei for subsequent crystal growth or by influencing the structural reorganisation in the glass, so that the desired crystalline phase will grow.[2,8]

The overall properties of glass ceramic systems are not a material constant, but depend on the percentages of crystalline and glassy phases formed and on the type, composition, shape and size of the crystals.[9] Hence, these materials display unique combinations of properties that can be tailored to meet specific requirements for a particular application.[2,4] The most commonly found features include high strength, hardness and resistance to wear, specific electrical properties, optical properties as translucency and other transmission characteristics, low and uniform thermal expansion and good dimensional stability.[2,3]

Compositions based on $Li_2O{\cdot}Al_2O_3{\cdot}SiO_2$ (LAS) are among the earliest glass ceramics developed, and have achieved great industrial and economical importance.[2,4,10] The main crystalline phases in this system are metastable solid solutions of the β-quartz or keatite structure.[4,7,11] Both β-quartz and keatite type lithium alumino-silicates adopt the tridimensional structure of SiO_2 polymorphs, with AlO_4 tetrahedra linked through their corners to SiO_4 tetrahedra in an ordered or disordered way, forming a tridimensional structure.[11] The Li^+ ions occupy cavities in the structure and provide

* Corresponding author.
E-mail address: jmf@cu.ua.pt (J.M.F. Ferreira).

0955-2219/01/$ - see front matter
PII: S0955-2219(00)00333-2

charge neutrality.[11] The most important crystalline phases in this system are β-eucryptite ($Li_2O{\cdot}Al_2O_3{\cdot}2SiO_2$), β-spodumene ($Li_2O{\cdot}Al_2O_3{\cdot}4SiO_2$) and β-petalite ($Li_2O{\cdot}Al_2O_3{\cdot}8SiO_2$).[7] In fact, their low or negative coefficients of thermal expansion (ranging from $-86\times10^{-7\circ}$ C^{-1} for β-eucryptite[3,12,13] to 9×10^{-7} $^{\circ}C^{-1}$ for β-spodumene[12]) enable tailoring glass ceramics with great resistance to thermal shock and good dimensional stability.[2] Additionally,[2,4] LAS-type glass ceramics can show high transparency and good mechanical properties (strength of ~150 MPa and elastic modulus of ~100 GPa for β-spodumene).[3]

The commercial glass ceramics in study have crystalline phases of the β-quartz solid solution type and were developed for applications were resistance to thermal shock or thermal gradients allied to optical transparency in the visible range are important features: Ceran® glass ceramic is produced for cooktop panels (tinted), while Robax® is used in windows and protective panels for domestic ovens and industrial furnaces (transparent).[4,12,14]

The present work aims to study the processing ability of LAS glass ceramics in order to evaluate its potential use for the fabrication of glass ceramic matrix composites by the powder route. Glass ceramic fabrication technology usually consists on the preparation of monolithic glass with appropriate base composition by traditional glass forming techniques, followed by controlled crystalisation.[2,4,5,8,15] Since crystallisation takes place after the forming step, this process renders glass ceramic parts with absolute non-porosity.[3,4,16] On the other hand, the production of glass ceramic parts by the powder route comprises a forming step followed by sintering and crystallisation heat treatments, allowing processing of complex shapes and the reduction of processing temperatures.[3,14] However, full densification by viscous flow may be difficult to achieve by the powder route due to the powders' large surface area for nucleation, which promotes crystallisation within each glass particle and an apparent increase in viscosity of the system.[3,17–21] The crystallisation and sintering behaviour, as well as the final properties of the glass-ceramic parts, are affected by the composition of the parent glass, the nucleating system and the crystallisation conditions.[14] Therefore, commercial LAS compositions successfully processed by glass melting technology (bulk processing) were chosen in order to minimise the number of experimental parameters.

2. Experimental procedure

2.1. Glass preparation and characterisation

Two commercial compositions supplied by Schott Glaswerke, Ceran® and Robax®, were used as starting raw materials. They were supplied in the form of glass ceramic plates, which were then crushed with a hammer, milled in a hammer mill, melted in silimanite crucibles (1450°C — 1 h) for complete homogenisation, and quenched in water. The so obtained glasses were then successively milled, as described in Table 1, in a hammer mill, agate mechanical mortar, planetary mill (Fritsch Pulverisette) and in an attrition mill (NFT-Netzsch). Resulting average particle sizes were measured by the sedimentation method (Sedigraph 5100, Micromeritics).

In order to confirm non-crystalinity, powder samples were analysed in a X-ray (CuK_α) powder difractometer (Rigaku Denki), with a scan speed of 3° and a step of 0.05°. The composition of both glass powders was determined by X-ray fluorescence (PW 14000, Philips) and atomic absorption spectrophotometry (Analyst 300, Perkin Elmer).

2.2. Heat treatment and characterisation

Characteristic glass temperatures such as glass transition (T_g), onset of crystallisation (T_o) and crystallisation maximum (T_p), were determined by differential thermal analysis (DTA). The measurements were performed in an alumina tubular furnace with Cromel-Alumel contact thermocouples, using calcined alumina as the reference material. DTA curves were recorded in air at different heating rates (10, 20, 30 and 40°C/min) up to the maximum temperature of 1200°C, using about 0.3 g of glass powders.

Several temperatures between T_g and T_o were tested to determine the most appropriate nucleation temperature (T_n). In each cycle the samples were heated at 50°C/min (sufficiently high rate to avoid nucleus formation during the heating step)[17,22,23] up to the chosen temperatures. After a dwelling time of 2 h, heating proceeded (at 30°C/min for Robax® and 40°C/min for Ceran®) until the appearance of the crystallisation peak. The nucleation times (t_n) were determined by heating the samples at 50°C/min up to the temperature

Table 1
Milling sequence of the glass powders

Type of mill	Milling conditions
Hammer mill	–
Agate mechanical mortar	60 min
Planetary mill	Agate mortar. Wet milling (60 vol.% glass powder + 40 vol.% ethanol), silicon nitride balls (Ø = 10.5 mm and 6.0 mm), 720 min at 4000 rpm.
Attrition mill	Teflon mortar. Wet milling (30 wt.% glass powder + 70 wt.% 2-propanol), YTZ balls (Ø = 2.1 mm), 250 min at 2000 rpm + 90 min at 4000 rpm + 60 min at 3000 rpm

T_n, with dwelling times varying between 2 and 7 h, followed by heating rates of 30°C/min for Robax® and 40°C/min for Ceran® until detection of the crystallisation peak.

The thermally treated samples were analysed by XRD to identify the crystalline phases formed during the DTA runs by matching X-ray diffraction patterns to JCPDS data. The crystal morphology was observed by scanning electron microscopy (Hitachi S-4100, Hitachi), on polished (1 μm diamond) and etched (4% hydrofluoric acid) surfaces.[1,16]

Dilatometry was used to determine the densification behaviour and the sintering onset (T_s) and completion (T_f) temperatures. The samples were fired at 10°C/min up to 1100°C. Parallelepiped (50 mm×5 mm×5 mm) specimens were formed by dry pressing (1GPa) 2.5 g of the ground powders, followed by isostatic pressing (2 GPa). Sintered densities were determined by the Archimedes method.

3. Results and discussion

3.1. Chemical composition

The average particle sizes of glass powders after the milling sequence shown in Table 1 were 1.79 μm for Robax® and 1.66 μm for Ceran. Both glasses are clearly non-crystalline as revealed by XRD and are composed by a large number of oxides each one performing a specific function (Table 2). These complex compositions are quite common in commercial low-expansion glass ceramics.[15] The composition of the base glass determines the crystalline phases formed during heat treatment, influences the melting, forming and crystallisation processes and the final properties of the glass ceramic.[2,15] Robax® contains a lower amount of colorants (transition metal oxides), which was confirmed by the supplier. The other compositional differences are in the range of the experimental error of the equipment used for the analysis.

Table 2
Identified oxides and loss on ignition (LOI) for the glasses in the study

Oxide	Robax® (wt.%)	Ceran® (wt.%)	Major function[15]
SiO_2	63.68	64.04	Forming h-quartz s.s.
Al_2O_3	21.82	21.34	
Li_20	3.95	3.94	
P_2O_5	0.10	0.10	
MgO	0.42	0.21	
ZnO	2.08	1.24	
TiO_2	2.18	2.07	Nucleating agents
ZrO_2	1.25	1.66	
Na_2O	1.45	1.35	Fluxing agents
BaO	1.97	2.28	
CaO	0.08	0.08	
MnO	0.08	0.21	Colouring agents
NiO	0.08	0.35	
CoO	0.01	0.26	
Cr_2O_3	0.04	0.04	
Fe_2O_3	0.42	0.62	
As_2O_3	0.07	0.05	Fining agent
LOI	0.2	0.1	

3.2. Nucleation and crystallisation from the glass

The purpose of a crystallisation heat treatment is to convert the original base glass into a microcrystalline material with improved properties.[16] This purpose is better attained for fine grained microstructures and, therefore, nucleation heat treatment should result in a high density of small crystals.[16]

DTA curves for Ceran® and Robax® are shown in Fig. 1. Both glasses exhibit similar thermal behaviours, summarised in Table 3. An endothermic effect corresponding to the glass transition temperature T_g is followed by a first exothermic peak due to crystallisation[24] and a second exothermic peak, less intense than the first one, attributed to crystalline phase transformations.[4,12,13] As would be expected, increasing heating rates result in a more pronounced displacement of the thermal effects towards higher temperatures, since heat transfer to the thermocouple junction is increasingly delayed.[25,26]

As referred to before, glass ceramic systems sinter by viscous flow of the glass above T_g. Once crystallisation is initiated the viscosity of the system sharply increases, hindering the completion of densification. The sintering

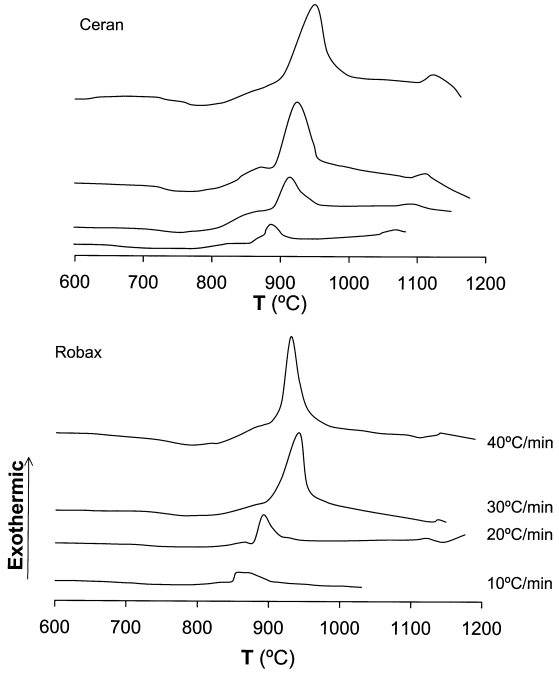

Fig. 1. DTA curves for Ceran® and Robax® at different heating rates.

Table 3
Characteristic temperatures for the glasses in the study (ϕ: heating rate; T_g: glass transition temperature; T_o: crystallisation onset; T_p/T_{p1}: maximum exothermic peak temperatures)

	ϕ (°C/min)	T_g (°C)	T_o (°C)	T_p (°C)	T_{p1} (°C)	T_0–T_g (°C)
Robax	10	690	852	873	1077	162
	20	709	878	894	1117	169
	30	722	894	924	1136	172
	40	736	905	944	1142	169
Ceran	10	695	871	896	1077	176
	20	704	886	923	1096	182
	30	708	900	934	1104	192
	40	718	912	941	1130	194

process must then take place within the softening range of the glass, preferably, and at the maximum allowed temperature.[3,19] Therefore, temperature and time corresponding to the maximum nucleation rate were determined for each glass using the method developed by Marotta and co-workers.[22,23] Plots of $(1/T_p)$ vs. T_n and $(1/T_p)$ vs. t_n were obtained for Robax® (Fig. 2) and Ceran® (Fig. 3). The maximum of each curve corresponds to the temperature and time of maximum nucleation rate, respectively. Analysis of the characteristic temperatures for each composition shows that the largest T_o–T_g ranges were obtained when heating was performed at 30°C/min for Robax® and 40°C/min for Ceran®. Hence, the most appropriate nucleation thermal cycles are heating at 40°C/min up to 782°C followed by a 5 h holding for Ceran® base glass, and heating at 30°C/min up to 776°C, followed by a 4h holding for Robax®. These thermal cycles were thus chosen in order to attain complete densification of the glass ceramic before the beginning of crystallisation.[3,13,15,19]

XRD revealed that heat-treating Robax at 30°C/min up to the temperature of the first DTA exothermic peak results in the formation of a lithium alumino-silicate of

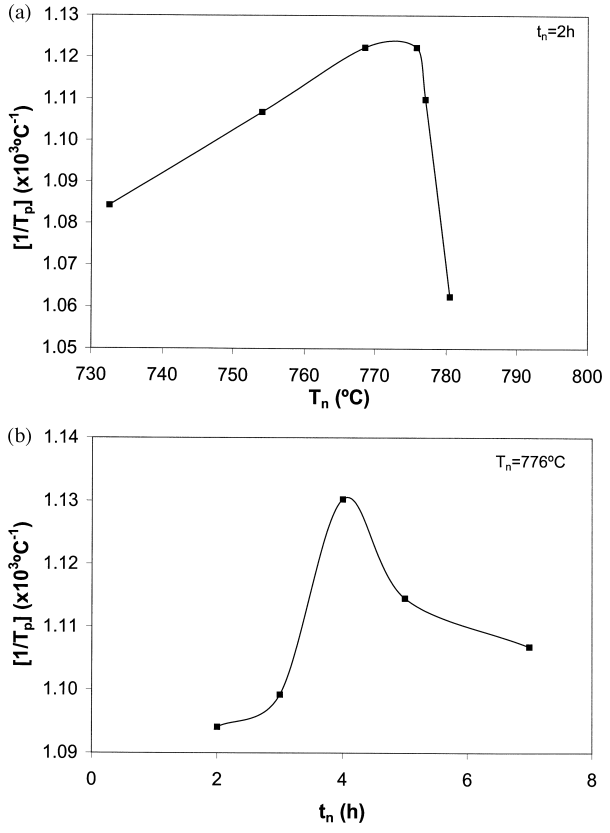

Fig. 2. Robax® glass-ceramic: maximum crystallisation peak temperature vs. (a) nucleation temperature (T_n); (b) nucleation time (t_n).

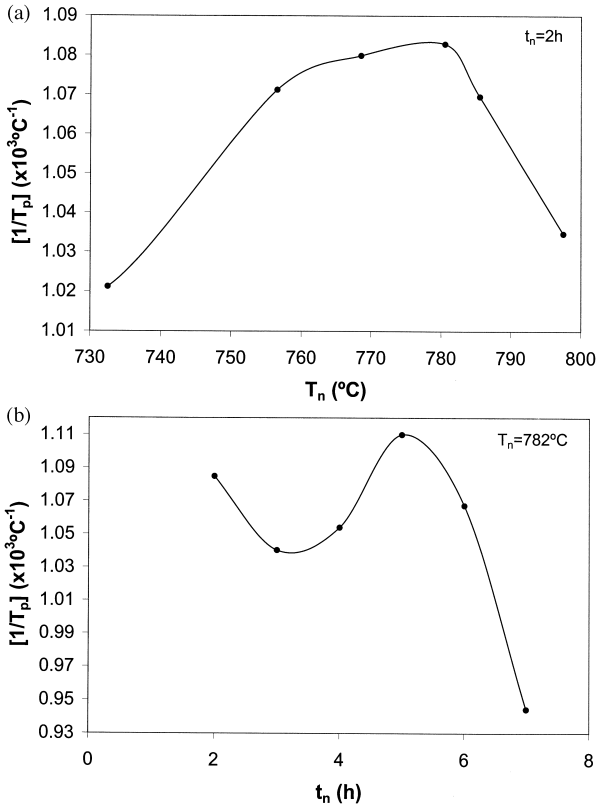

Fig. 3. Ceran® glass-ceramic: maximum crystallisation peak temperature vs. (a) nucleation temperature (T_n); (b) nucleation time (t_n).

hexagonal symmetry ($Li_xAl_xSi_{1-x}O_2$) and an unidentified phase (Fig. 4a). The crystalline phases identified after heat-treating the same glass up to the second exothermic peak were β-spodumene ($LiAlSi_2O_6$) and SiO_2, both of tetragonal symmetry, together with the unidentified phase (Fig. 4b). These results agree with those reported by Pannhorst,[24] which states that the exothermic peak with onset around 1000°C refers to phase transformation from β-quartz s.s. (hexagonal symmetry) to keatite s.s. (tetragonal symmetry).[4,12,13] Because of the fine grain microstructure, glass ceramics containing β-quartz s.s. are, in most cases, transparent. Keatite s.s. crystals are large, thus the strong scattering from the crystallites results in opaque glass ceramics in the visible spectrum.[14,27] Additionally, β-quartz s.s. glass ceramics have CET ranging from -20×10^{-7} K^{-1} to 5×10^{-7} K^{-1}, while keatite s.s. exhibits a CET between 10 and 20×10^{-7} K^{-1}.[15] In order to obtain LAS glass ceramics with low CET (resistance to thermal shock implies CET lower than $\sim5\times10^{-7}K^{-1}$) and high transparency, appropriate for their specific applications, the phase transformation from β-quartz s.s. to keatite s.s. is avoided in commercial glass ceramics.[4,15]

The same crystalline phases were identified for Ceran® heated at 40°C/min. Nevertheless, the corresponding X-ray diffraction peaks have comparatively smaller intensities, indicating lower degree of crystallinity. Since also minor constituents of the parent glass can have a profound effect on the composition and volume fraction of the phases formed,[2] the colouring agents present in Ceran® base glass are thought to retard crystallisation. This is in good agreement with the work of Barbieri et al.[28] that states that the addition of NiO or CoO to LAS glass compositions acts on the crystallisation rate, although does not alter the crystalline phases formed.

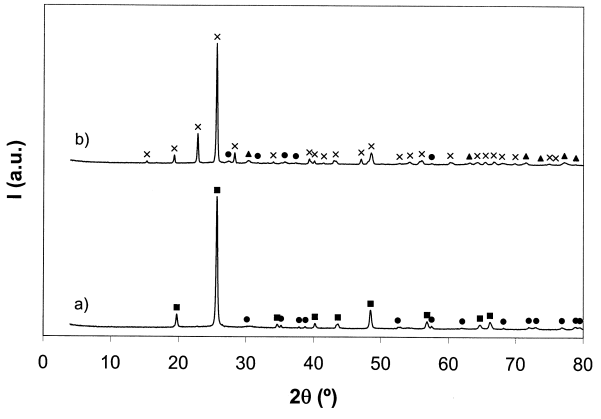

Fig. 4. X-ray diffraction patterns for Robax® heated at 30°C/min: (a) up to the first maximum exothermic peak temperature; (b) up to the second maximum exothermic peak temperature. (■: lithium aluminosilicate, $Li_xAl_xSi_{1-x}O_2$; ×: β-spodumene, $LiAlSi_2O_6$; ▲: silica (tetragonal); ●: unidentified phase).

Microstructures obtained by heating Robax® at 30°C/min up to each DTA exothermic peak are shown in Fig. 5. A sample corresponding to the first exothermic peak (Fig. 5a) shows an etched crystalline matrix mainly constituted by nanometric spherical crystallites and porous areas that may result from dissolution of the residual glassy regions. This nanometric crystalline phase is thought to correspond to the non-stoichiometric lithium alumino-silicate ($Li_xAl_xSi_{1-x}O_2$) identified by XRD. A small amount of other spherical crystals of about 1 μm can also be observed in Fig. 5a. Fig. 5b suggests that this crystalline phase develops by further heating the sample up to the second DTA exothermic peak, appearing as large size crystals which, according to the XRD results, are β-spodumene ($LiAlSi_2O_6$).

3.3. Kinetics of nucleation and crystal growth

DTA results were treated in order to determine the crystallisation kinetic parameters, order of reaction n and activation energy E. The order of the crystallisation

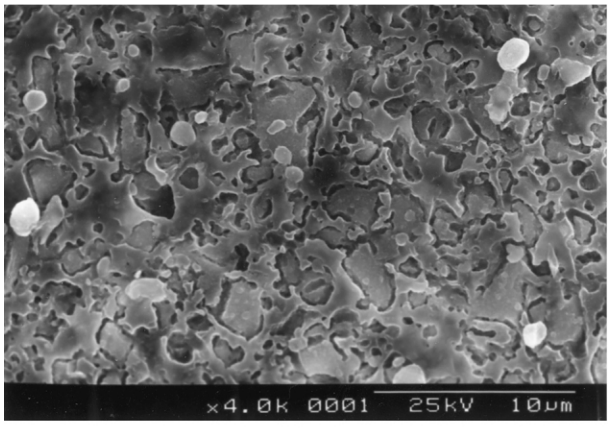

(a)

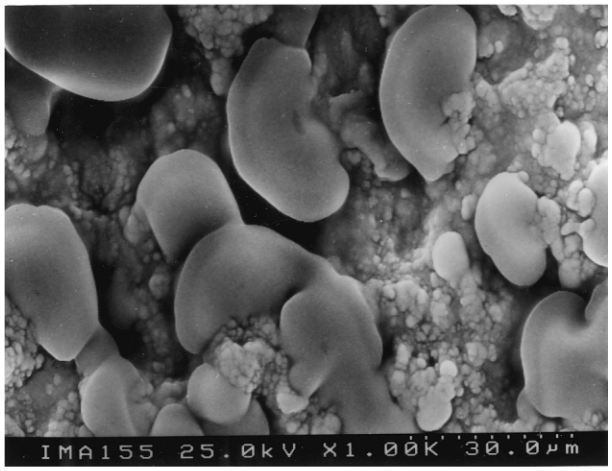

(b)

Fig. 5. Microstructure of the Robax® glass-ceramic heated at 30°C/min: (a) up to the first maximum exothermic peak temperature (924°C); (b) up to the second maximum exothermic peak temperature (1136°C).

reaction (Avrami parameter) was determined using the method proposed by Ozawa:[3,17]

$$-n = \left|\frac{\mathrm{d}[l\mathrm{n}(-\,l\mathrm{n}(1-x))]}{\mathrm{d}(l\mathrm{n}\phi)}\right|_T \quad (1)$$

where the crystallised volume fraction x is obtained at the same temperature T from the crystallisation exothermic taken at different heating rates ϕ (in practice, x is the ratio of the fraction area at temperature T to the total area of the crystallisation peak). Ozawa's plots from Eq. (1) at 891°C (Fig. 6) render $n \cong 2.4$ for Robax® and $n \cong 1.5$ for Ceran®. Since $n = 1$ when surface crystallisation dominates and $n = 3$ when bulk crystallisation prevails,[17] those results indicate that surface and bulk crystallisation occur simultaneously in both glasses, as expected,[2,29] (n between 1 and 3). Nevertheless, the contribution of bulk nucleation is somehow greater in Robax® than in Ceran® glasses, in good agreement with its slightly larger particle size.

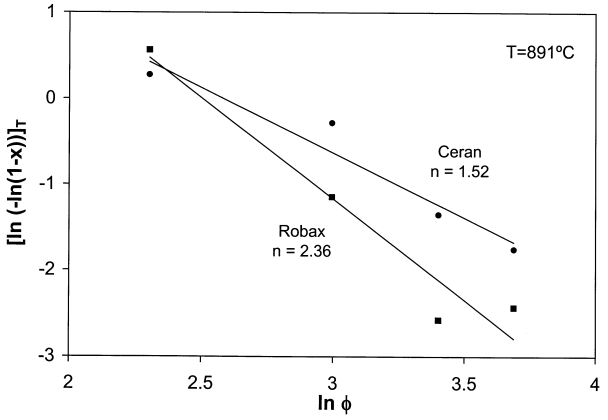

Fig. 6. Ozawa plots for determining crystallisation reaction order. ■ Robax® (correlation coefficient = 0.972). ● Ceran ®(c.c. = 0.969). (Crystallised volume fraction taken at 891°C).

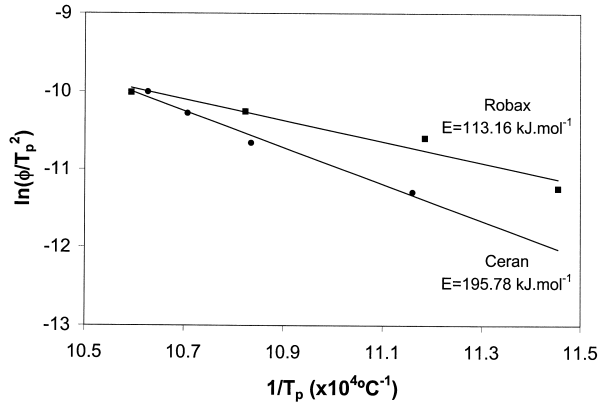

Fig. 7. Kissinger plots for determining activation energy. ■ Robax® (c.c. = 0.974) and ● Ceran® (c.c. = 0.991).

As for determination of activation energy for nucleation and crystal growth, the method developed by Kissinger was used:[3,17]

$$l\mathrm{n}\frac{\pi}{T_\mathrm{p}^2} = \mathrm{constant} - \frac{E}{RT_\mathrm{p}} \quad (2)$$

where R is the gas constant and T_p the temperature at the maximum of the crystallisation peak. The plot of $\ln(\phi/T_\mathrm{p}^2)$ vs. $1/T_\mathrm{p}$ was adjusted to a straight line, whose slope yields the activation energy for crystallisation (Fig. 7). The determined activation energies are 113.2 kJ/mol for Robax® and 195.8 kJ/mol for Ceran®. These results are consistent with Ceran®'s minor degree of crystallinity.

3.4. Sintering behaviour

The percentage linear shrinkage vs. temperature for Robax® and Ceran® base glasses is represented in Fig. 8. The total shrinkage (Table 4) is higher for Ceran® (20.6%) than for Robax® (17.8%). Since the mean particle size and particle size distributions are similar, the factors determining the densification behaviour of the powders are the parent glasses' viscosity and crystallisability.[13,14] Hence, it's suggested that Ceran®'s greater sinterability derives from the powders' composition. Small compositional differences between both glasses are observed. Ceran® contains a higher total amount of colouring agents (+0.85 wt.%), which together with a slight excess of fluxing agents and a

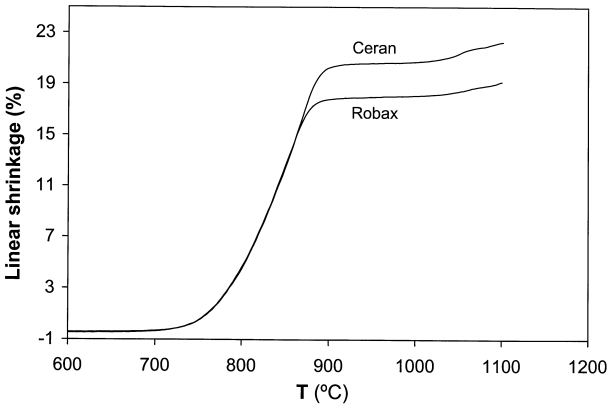

Fig. 8. Dilatometry results for Ceran® and Robax® heated at 10°C/min up to 1100°C.

Table 4
Dilatometry results for Robax® and Ceran®. (T_s: start sintering temperature; T_f: completion sintering temperature)

Composition	Shrinkage (%)	T_s (°C)	T_f (°C)
Robax®	17.8	777	869
Ceran®	20.6	774	893

slight deficiency in alumina, may either contribute to decrease the viscosity of the system, or to work as glass network forming oxides, delaying crystallisation onset.[13]

Both compositions show rapid shrinkage above approximately 770°C. The sinterability range of both powders is quite narrow, with sintering completion at 869°C for Robax^{bhs} and 893°C for Ceran®. Density measurements show that at the crystallisation onset (879°C for Robax® and 946°C for Ceran®, when heated at 10°C/min.) the powders are only partially densified. At these temperatures, Ceran® and Robax® present 86.1±2.1% and 78.6±2.3% of the theoretical density, respectively. Above those temperatures, the resulting increase in viscosity hinders the viscous sintering process, and other sintering mechanisms (solid or liquid phase processes) come into play, preventing the attainment of fully densified glass ceramics by pressureless sintering.[19]

4. Conclusions

1. The compositions of the studied commercial LAS glasses differ mainly on the amount of colouring agents (transition metal oxides), which, together with other slight compositional differences significantly affect the crystallisation and densification behaviour of the powders.
2. On heating, the glass powders first crystallise into β-quartz s.s., which then transforms into β-spodumene and silica at higher temperatures. An unidentified crystalline phase was found in both cases. XDR peaks are less intense in the case of Ceran®, indicating a lower degree of crystallinity. As a consequence, Ceran® glass attains higher densification levels.
3. When heat-treated at 10°C/min, both compositions sinter only partially before crystallisation begins hindering full densification by pressureless sintering.

Acknowledgements

The authors acknowledge the FCT (Portuguese Foundation for Science and Technology) for the grant to M.G. in the frame of Praxis XXI program.

References

1. Lee, K. H., Hirschfeld, D. A. and Brown, J. J., In situ reinforced glass ceramic in the lithia-alumina-silica system. In *Ceramic Transactions, vol. 30: Nucleation and Cristalization in Liquids and Glasses*, ed. M. C. Weinberg. The American Ceramic Society, Ohio, 1993, pp. 293–300.
2. Partridge, G., An overview of glass ceramics: Part 1 — development and principal bulk applications. *Glass Technology*, 1994, **35**(3), 116–127.
3. Sung, Y.-M., Dunn, S. A. and Koutsky, J. A., The effect of boria and titania addition on the crystallization and sintering behaviour of Li_2O–Al_2O_3–$4SiO_2$ glass. *J. Eur. Ceram. Soc.*, 1994, **14**, 455–462.
4. Scheidler, H. and Rodek, E., Li_2O–Al_2O_3–SiO_2 glass-ceramics. *Ceram. Bull.*, 1989, **68**(11), 1926–1930.
5. James, P. F., Glass ceramics: new compositions and uses. *J. Non-Cryst. Sol.*, 1995, **181**, 1–15.
6. Hsu, J.-Y. and Speyer, R. F., Comparison of the effects of titania and tantalum oxide nucleating agents on the crystallization of Li_2O–Al_2O_3–$6SiO_2$ glasses. *J. Am. Ceram. Soc.*, 1989, **71**(12), 2334–2341.
7. Strnad, Z. Glass Ceramic Materials: Liquid Phase Separation, Nucleation and Cristallization in Glasses. Amsterdam: Elsevier, 1986.
8. Fernandez Navarro, J. M. El Vidrio: Constitución, Fabricatión, Propriedades. Madrid: CSIC, 1985.
9. Scheidler, H. and Thürk, J., The ceran-top-system®: high tech appliance for the kitchen. In *Low Thermal Expansion Glass Ceramics*, ed. H. Bach. Springer-Verlag, Berlin, 1995, pp. 51–60.
10. Pannhorst, W. An overview. In: *Low Thermal Expansion Glass Ceramics*, H. Bac. Springer-Verlag, Berlin, 1995, pp. 1–12.
11. Müller, G., Structure, composition, stability and thermal expansion of high-quartz and keatite type alumino-silicates. In *Low Thermal Expansion Glass Ceramics*, ed. H. Bach. Springer-Verlag, Berlin, 1995, pp. 13–25.
12. Pannhorst, W. E., Low expansion glass ceramics: review of the glass ceramics ceran and zerodur and their applications. In *Ceramic Transactions Nucleation and Cristalization in Liquids and Glasses, vol. 30*, ed. M. C. Weinberg. The Americam Ceramic Society, Ohio, 1993, pp. 267–276.
13. Knickerbocker, S., Tuzzolo, M. R. and Lawhorne, S., Sinterable β-spodumene glass ceramics. *J. Am. Ceram. Soc.*, 1989, **72**(10), 1873–1879.
14. Naβ, P., Rodek, E., Schildt, H. and Weinberg, W., Development and production of transparent colourless and tinted glass ceramics. In *Low Thermal Expansion Glass Ceramics*, ed. H. Bach. Springer-Verlag, Berlin, 1995, pp. 60–79.
15. Shyu, J. J. and Lee, H. H., Sintering, crystallization and properties of B_2O_3/P_2O_5 doped $Li_2O{\cdot}Al_2O_3{\cdot}4SiO_2$ glass-ceramics. *J. Am. Ceram. Soc.*, 1995, **78**(8), 2161–2167.
16. McMillan, A., *Glass-Ceramics*. Academic Press, London, 1964.
17. Ray, C. S. and Day, D. E., Nucleation and crystallization in glasses as determined by DTA. In *Ceramic Transactions Nucleation and Cristalization in Liquids and Glasses, vol. 30*, ed. M. C. Weinberg. The American Ceramic Society, Ohio, 1993, pp. 207–223.
18. Scherer, G. W. and Uhlmann, D. R., Effects of phase separation on crystallization behaviour. *J. Non-Cryst. Sol.*, 1976, **21**, 199–213.
19. Ferraris, M. and Verné, E., Viscous phase sintering of particle reinforced glass matrix composites. *J. Eur. Ceram. Soc.*, 1996, **16**, 421–427.
20. Anseau, M. R., Cambier, F. and Leriche, A., Vitrification. In *Concise Encyclopedia of Advanced Ceramic Materials*, ed. R. J. Brook. Pergamon Press, Oxford, 1991, pp. 506–509.
21. German, R. M. Fundamentals of sintering. In *Engineered Materials Handbook: vol. 4: Ceramics and Glasses*. ASM, 1991, pp. 260–269.
22. Marotta, A., Buri, A. and Branda, F., Nucleation in glass and differential thermal analysis. *J. Mater. Sci.*, 1981, **16**, 341–344.
23. Cioffi, R., Pernice, P., Aronne, A. and Marotta, A., Nucleation and crystal growth in a fly ash derived glass. *J. Materz. Sci.*, 1993, **28**, 6591.

24. Pannhorst, W., Glass ceramics based on lithium-alumino-silicate solid solution crystals. In *Low Thermal Expansion Glass Ceramics*, ed. H. Bach. Springer-Verlag, Berlin, 1995, pp. 39–49.
25. Todor, D. N., *Thermal Analysis of Minerals*. Abacus Press, Kent, 1976.
26. Speyer, R. F., *Thermal Analysis of Materials*. Dekker, NY, 1994.
27. Schiffer, U., Nucleation in parent glasses for lithia alumino-silicate glass ceramics. In *Low Thermal Expansion Glass Ceramics*, ed. H. Bach. Springer-Verlag, Berlin, 1995, pp. 25–39.
28. Barbieri, L., Bruni, S., Cariati, F., Leonelli, C., Manfredini, T., Pellacani, G. C. and Siligardi, C., Coloring transition polyvalent cations in $Li_2O{\cdot}Al_2O_3{\cdot}4SiO_2$ glass-ceramics. In *Third Euro-ceramics, V.2*, ed. P. Dúran and J. F. Fernández. Faenza Editrice Ibérica, Spain, 1993, pp. 1199–1204.
29. Matusita, K. and Saka, S., Kinetic study on crystallization of glass by differencial thermal analysis: criterion on application of Kissinger plot. *J. Non-Cryst. Sol.*, 1980, **38–39**, 741–746.